Brillouin-scattering study of propylene carbonate: An evaluation of phenomenological and mode coupling analyses

Alexander Brodin,[1] Martin Frank,[1,2] Sabine Wiebel,[2] Guoqing Shen,[1,*] Joachim Wuttke,[2] and H. Z. Cummins[1]
[1]*Physics Department, City College of the City University of New York, New York, New York 10031*
[2]*Physik-Department E13, Technische Universität München, 85747 Garching, Germany*
(Received 29 August 2001; published 2 May 2002)

Brillouin-scattering spectra of the molecular glass-forming material propylene carbonate (PC) in the temperature range 140 K to 350 K were analyzed using both the phenomenological Cole-Davidson memory function and a hybrid memory function consisting of the Cole-Davidson function plus a power-law term representing the critical decay part of the fast β relaxation. The spectra were also analyzed using the extended two-correlator schematic mode-coupling theory (MCT) model recently employed by Götze and Voigtmann to analyze depolarized light backscattering, dielectric, and neutron-scattering spectra of PC [Phys. Rev. E **61**, 4133 (2000)]. We assess the ability of the phenomenological and MCT fits, each with three free fitting parameters, to simultaneously describe the spectra and give reasonable values for the α-relaxation time τ_α.

DOI: 10.1103/PhysRevE.65.051503 PACS number(s): 64.70.Pf, 78.35.+c, 67.40.Fd

I. INTRODUCTION

When a liquid is cooled through its melting temperature T_M towards its glass-transition temperature T_G, the characteristic time τ_α for the relaxation of fluctuations increases dramatically, from $\sim 10^{-12}$ s at T_G+100 K to $\sim 10^2$ s at T_G. During the past decade, it has been recognized that structural relaxation dynamics take place on different time scales, with the α-relaxation process, characterized by the relaxation time τ_α, being the final stage of the approach to equilibrium.

Brillouin-scattering spectroscopy is one of many experimental techniques that has been employed to study the temperature-dependent dynamics of structural relaxation in a wide variety of glass-forming materials. The evolution of the Brillouin spectrum with temperature reflects the interaction of longitudinal sound waves ($q \sim 10^5$ cm^{-1}) with structural relaxation. Typically, as T decreases from above the melting temperature T_M to below the glass-transition temperature T_G, the Brillouin linewidth $\Delta\omega_B$, which is proportional to the damping rate for the sound wave, first increases, passes through a maximum, and then decreases again, while the Brillouin peak position ω_B shifts monotonically to higher frequencies. This increase occurs predominantly in the temperature range where $\Delta\omega_B$ is largest, corresponding to $\omega_B\tau_\alpha \approx 1$.

The analysis of these spectra has usually been carried out using generalized hydrodynamics methods. Following a procedure introduced by Mountain [1], a frequency-dependent component is added to the longitudinal viscosity by introducing a viscosity memory function $m(t)$. Generally, acceptable fits can be obtained using an exponential or stretched-exponential empirical memory function $m(t)$ (or a Cole-Davidson memory function $m[\omega]$), with the relaxation time $\tau_\alpha(T)$ treated as an adjustable fitting parameter. However, at low temperatures, the $\tau(T)$ values determined from such α-relaxation-only fits are usually found to increase much more slowly with decreasing T than the values determined with other techniques such as dielectric spectroscopy or ultrasonics.

In view of this disagreement *despite* the excellent fits, a question naturally arises as to whether or not Brillouin-scattering spectroscopy can reveal useful information about structural relaxation dynamics. In the present paper, we attempt to answer this important question. The goal is not to obtain better fits by adding additional parameters to the memory function; we carry out all fits with just three free fitting parameters, making use of other data to fix the remaining parameters where possible.

We first address the problem of the inconsistency in determining $\tau_\alpha(T)$. Several authors have proposed procedures for extending the memory function to include the ''fast-relaxation'' processes that contribute to $m[\omega]$ at frequencies above the region of the α relaxation [2–10]. With the additional fast-relaxation included, excellent fits can be obtained with the α-relaxation time τ_α constrained to increase much more rapidly with decreasing temperature than it does with α-relaxation-only models, consistent with other experimental measurements. However, this approach does not reliably provide values for τ_α, nor does it explain the origin of the structural relaxation dynamics that it describes. Furthermore, various authors have chosen quite different empirical fitting functions and have usually obtained good fits to Brillouin spectra, suggesting that this procedure is not able to distinguish effectively between different models.

Another approach to the analysis of Brillouin-scattering spectra utilizes the mode-coupling theory (MCT) in which the slowing down of structural relaxation with decreasing T arises naturally from nonlinear interactions among density fluctuations. A major advantage of the MCT approach is that both the α and β (fast) regions of the relaxation dynamics occur spontaneously in the solutions of the MCT equations for the particle density autocorrelation function $\phi_q(t)$.

*Present address: Physics Department, Emory University, Atlanta, GA 30322.

TABLE I. Properties of propylene carbonate.

Property	Value
Formula	$C_4H_6O_3$
Molecular weight	102.09
T_{boil}	513 K
T_M	218 K
T_G	160 K
T_C (MCT crossover temperature)	185 ± 5 K[a]
λ (MCT exponent parameter)	0.75 ± 0.3[a]
Density $\rho(T)$	$1.541-(1.148\times10^{-3})T$ (g/cm^3)[b]
Refractive index $n_D(T)$	$1.5314-(3.752\times10^{-4})T$[b]
Sound velocity $C_0(T)$	$2.5075\times10^5-361.2T$ cm/sec[c]
β_K (Kohlrausch stretching coefficient) (depolarized light scattering)	0.77 ± 0.05[c]
β_{CD} (Cole-Davidson stretching coefficient) (depolarized light scattering)	0.68[c]
m (fragility index)	104[f]

[a]Reference [15].
[b]Reference [35].
[c]Reference [8].
[d]Reference [18].
[e]Reference [36].
[f]Reference [37].

A convenient schematic MCT model, initially introduced by Sjögren [11], uses two correlators: $\phi(t)$ for the ''system'' and $\phi_s(t)$ for the ''probe,'' i.e., the variable being measured in a particular experiment. This model was successfully used to analyze depolarized light-scattering spectra of glycerol [12] and orthoterphenyl (OTP) [13]. Ruffl*é et al.* [14] showed that Brillouin-scattering spectra of $NaLi(PO_3)_2$ could also be analyzed with the Sjögren model, using parameters for the system correlator $\phi(t)$ determined from inelastic neutron-scattering spectra.

Recently, Götze and Voigtmann have extended the Sjögren model by including hopping parameters in the equations of motion for both $\phi(t)$ and $\phi_s(t)$, which allows the analysis to be extended to low temperatures where relaxation is dominated by activated hopping processes. They analyzed dielectric, depolarized light-scattering, and neutron-scattering data for the molecular glass-forming material propylene carbonate (PC), using a single set of system parameters for $\phi(t)$, optimized simultaneously for all the experiments [15]. This result suggests the possibility of analyzing PC Brillouin-scattering spectra using the system parameters for $\phi(t)$ already determined by Götze and Voigtmann. Moreover, if the probe hopping parameter, frequency, and damping constant are taken as fixed by the depolarized light-scattering fits, then the analysis will include only one adjustable MCT fitting parameter, the coupling constant V_s, which determines the strength of coupling between $\phi(t)$ and $\phi_s(t)$. The fits should then *simultaneously* describe the Brillouin spectra and also determine the value of the structural relaxation time τ_α. Such an analysis could provide a stringent test of the utility of MCT for the analysis of Brillouin-scattering spectra. A test of this procedure was the principal motivation for the present Brillouin-scattering study of PC.

The paper is organized as follows. We describe the experiments in Sec. II. We first analyze the data in Sec. III using a conventional α-relaxation-only Cole-Davidson (CD) function, and then in Sec. IV, with the hybrid model, which adds a term $B\omega^a$ to the Cole-Davidson function to approximate the fast-β-relaxation process. (A preliminary version of the CD and hybrid fits was presented by Frank [16].)

In Sec. V we present our analysis of the spectra with the two-correlator extended schematic MCT approach. Discussion and conclusions are presented in Sec. VI, including a brief evaluation of the ability of these and related approaches to extract meaningful information about structural relaxation dynamics from the analysis of Brillouin-scattering spectra.

II. EXPERIMENT

A. Material

Propylene carbonate ($T_G=160$ K) is a molecular glass-forming material that has been extensively studied with a wide range of experimental techniques including Brillouin scattering [17,8]. In Table I we list the principal properties of PC that are relevant for the present study.

A recent dielectric spectroscopy study of PC by Schneider *et al.* [18] determined the complex dielectric constant $\epsilon(\omega)$ over a frequency range of 18 decades for temperatures from 153 K to 293 K. Cole-Davidson fits to the α peaks in the $\epsilon''(\omega)$ spectra produced the $\tau_\alpha^\epsilon(T)$ values shown in Fig. 1 by the open circles. Schneider *et al.* carried out fits to these values with several empirical fitting functions. Their extended free-volume fit is shown in Fig. 1 by the upper line.

Du *et al.* [8] fit the α peaks in the $\chi''(\omega)$ spectra, obtained from their depolarized PC backscattering spectra, with a Kohlrausch function. The resulting τ_α^{DLS} values, shown in Fig. 1 by squares, have a temperature dependence similar to the dielectric $\tau_\alpha^\epsilon(T)$ although they are approximately three times smaller.

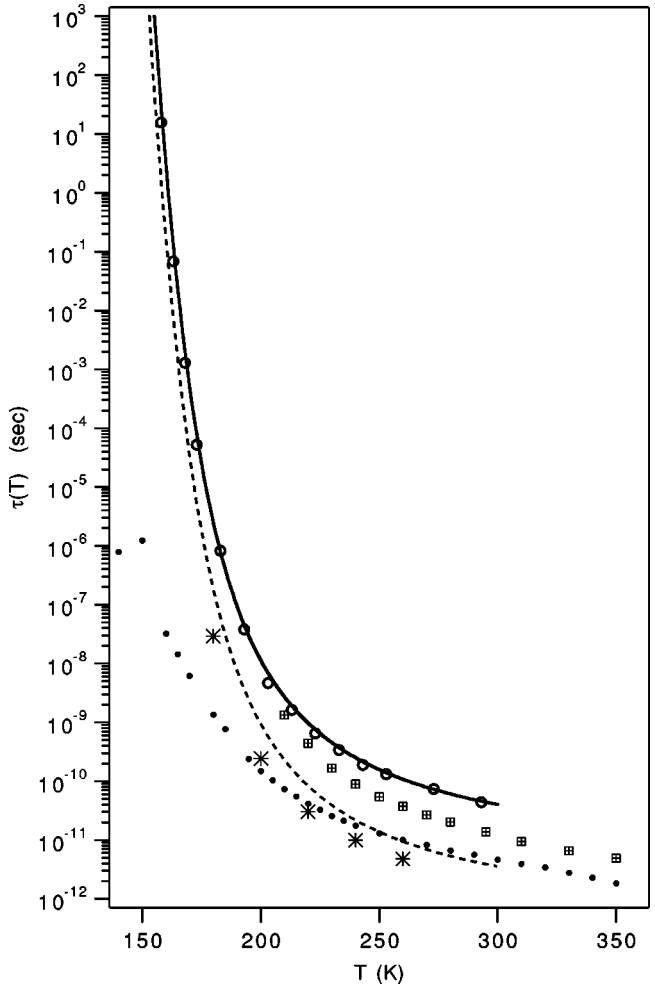

FIG. 1. Propylene carbonate (PC) relaxation time $\tau_\alpha(T)$. Open circles and upper solid line: dielectric measurements and extended free-volume fit [18]. Squares: depolarized light-scattering spectra [8]. Solid circles: Brillouin scattering $\tau_\alpha^{CD}(T)$ from Cole-Davidson fits (Sec. III). Lower line: dielectric free-volume fit multiplied by 0.085 to match Brillouin $\tau_\alpha(T)$ in the region of the maximum Brillouin linewidth. $*$: τ_α^{MCT} obtained from the extended schematic MCT fits (Sec. V).

The analysis of our Brillouin-scattering spectra using a Cole-Davidson memory function, described in the following section, resulted in the τ_α^{CD} values shown by the solid circles in Fig. 1. As mentioned in the Introduction, at low temperature these values do not increase as rapidly with decreasing temperature as the dielectric and backscattering results, suggesting that the Cole-Davidson function provides an incomplete representation of structural relaxation. [At $T=T_G \sim 160$ K, τ_α^{CD} has only reached ~ 30 ns, while typically $\tau_\alpha(T_G)$ is ~ 100 s.]

In our 90° PC Brillouin-scattering experiment, the maximum Brillouin linewidth occurs at $T \sim 230$ K. At that temperature the peak of the α relaxation coincides with the Brillouin line, so $\omega_B \tau_\alpha^{LA} \approx 1$, which gives τ_α^{LA} (230 K) $\sim 3.2 \times 10^{-11}$ s, a value ~ 12 times smaller than the τ_α^{ϵ} of Schneider *et al.* The difference presumably arises from the fact that τ_α^{LA} characterizes longitudinal displacement dynamics while $\tau_\alpha^{\varepsilon}$ characterizes orientational dynamics. In Fig. 1, the lower line is the free-volume fit of Schneider *et al.* divided by a factor of 11.75 to match τ_α^{LA} in this region,

$$\log_{10}(\tau_\alpha^{LA}) = -A + B/\{T - T_0 + [(T-T_0)^2 + CT]^{1/2}\} \quad (1)$$

with $A=12.56$, $B=309$, $C=4.82$, and $T_0=162$ K (τ_α^{LA} in seconds). In constructing memory functions for data analysis beyond the Cole-Davidson model, we will use Eq. (1) to fix the α-relaxation time of the longitudinal acoustic mode τ_α^{LA}.

B. Sample preparation

Propylene carbonate (anhydrous, 99.7%) was purchased from Sigma-Aldrich. PC was loaded in a glove box under dry nitrogen atmosphere into a distillation flask fitted with a stopcock. The flask was then transferred to a vacuum distillation system and distilled at ~ 110°C into glass sample cells that were flame sealed under vacuum. A sample cell was installed in an Oxford LN2 coldfinger cryostat with an ITC-4 temperature controller for the Brillouin-scattering experiments.

C. Brillouin-scattering experiments

Spectra were collected in both 90° VV (vertical-vertical, polarized) geometry and 174° VH (vertical-horizontal, depolarized) near-backscattering geometry with a Sandercock 6-pass tandem Fabry-Perot interferometer at temperatures from 140 K to 350 K in 5-K or 10-K steps. The 514.5-nm single-mode argon laser power at the sample was typically 170 mW. The interferometer finesse was ~ 90; its contrast was better than 10^7. Complete sets of spectra were collected with mirror separations $d=2$, 5, and 10 mm corresponding to free spectral ranges of 75, 30, and 15 GHz for VV, and $d=2$ mm and 10 mm for VH. Spectra were accumulated during (1–2)-h runs. For the $d=10$ mm separation spectra two 2-h runs were collected and averaged to improve the signal-to-noise ratio. In Fig. 2 we plot the Stokes side of the three VV spectra (a) and the two VH spectra (b) for $T=220$ K. (The dark counts have already been subtracted.)

In order to test for possible experimental artifacts, PC Brillouin spectra at several temperatures were collected at both the Technical University of Munich and at the City College of New York with different samples, different tandem Fabry-Perot spectrometers, and different experimental procedures. The spectra obtained were in good agreement.

D. Data reduction: Extraction of the density fluctuation spectra $I_{ISO}(\omega)$

The VV polarized Brillouin spectra contain contributions from density fluctuations $[I_{ISO}(\omega)]$ and also from orientational dynamics and collision-induced scattering $[I_{ANI}(\omega)]$. Depolarized (VH) backscattering spectra are due to $I_{ANI}(\omega)$ only and can, therefore, be used to remove the $I_{ANI}(\omega)$ contribution from the VV spectra.

Fioretto *et al.* [19,6] have carried out the subtraction by combining spectra obtained with different mirror separations

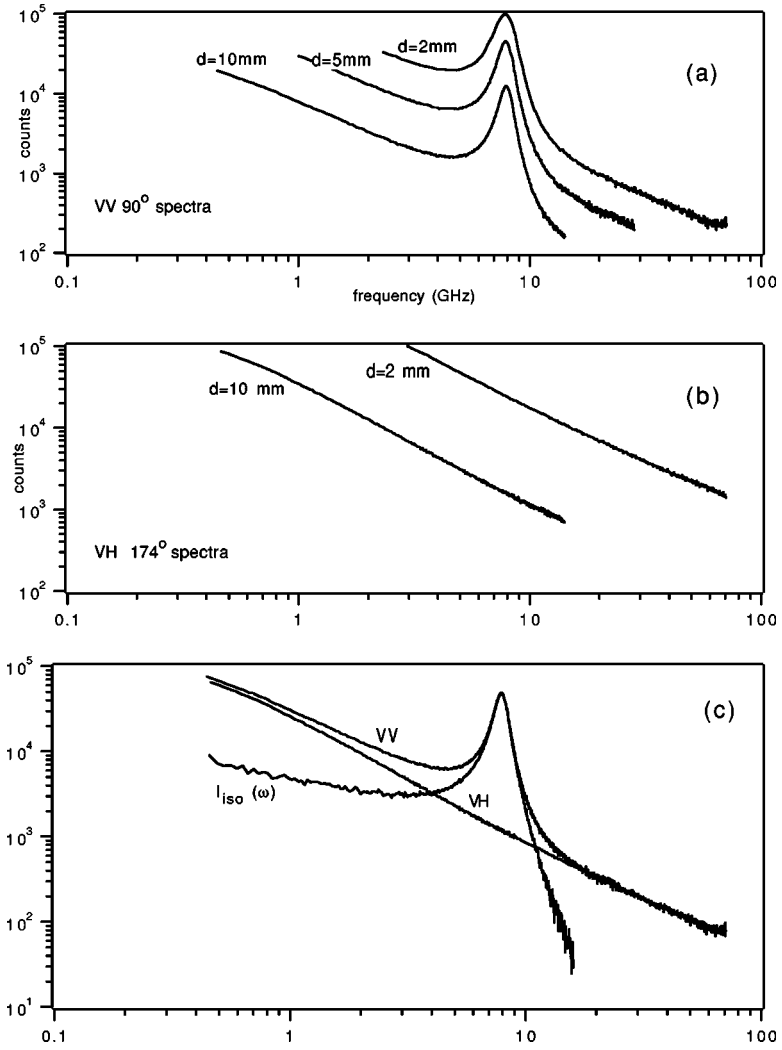

FIG. 2. (a) Stokes sides of 220-K PC 90° VV Brillouin spectra with $d=2, 5$, and 10 mm. (b) 174° VH spectra with $d=2$ mm and 10 mm. (c) The composite 90° VV spectrum obtained by shifting the 2-mm and 5-mm spectra of (a) to optimize overlap with the 10-mm spectrum, the composite VH spectrum obtained similarly and then shifted to optimize overlap with the VV spectrum for frequencies above 30 GHz, and the difference spectrum $I_{ISO}(\omega)$ obtained by subtraction. The background from dark counts has already been subtracted in the spectra of (a) and (b).

to obtain broadband VV and VH spectra, and scaling the VH spectra to overlap the VV spectra for frequencies above ~ 40 GHz where $I_{ISO}(\omega)$ should be negligible. Subtracting the scaled $I_{VH}(\omega)$ from the $I_{VV}(\omega)$ then provides $I_{ISO}(\omega)$. We have also followed this procedure.

The Stokes sides of the $d=2$ and 10 mm 220-K VV spectra, shown in Fig. 2(a), were rescaled vertically to optimize overlap with the $d=5$ mm spectrum, producing the composite 90° $I_{VV}(\omega)$ spectrum shown in Fig. 2(c). The $\theta=174°$ $I_{VH}(\omega)$ spectra were similarly combined, and the composite I_{VH} spectrum was again scaled vertically to match the I_{VV} spectrum in the (30–50)-GHz region. Finally, the scaled I_{VH} spectrum was subtracted from the I_{VV} spectrum to produce the difference spectrum $I_{ISO}(\omega)$ as shown in Fig. 2(c).

The full set of $I_{ISO}(\omega)$ spectra for temperatures from 140 K to 350 K obtained with this procedure is shown in Fig. 3. For each set of VV spectra, we also recorded an instrument profile spectrum with $d=10$ mm. The full width at half maxmimum of the instrumental profile was typically 0.17 GHz. To reduce additional Brillouin peak broadening due to the finite input aperture (which leads to collecting light scattered at slightly different angles), the input aperture was reduced sufficiently to decrease the additional broadening at the Brillouin frequency to less than the instrumental width. This additional geometrical broadening (typically $\lesssim 0.13$ GHz) was then calculated for every temperature from the known collection geometry and convoluted into the instrument function. In the fitting procedures described in this paper, the instrument function so obtained was convoluted with the theoretical spectrum for comparison with the $I_{ISO}(\omega)$ spectrum. The fits were carried out with a conventional nonlinear least-squares fitting program (NLLSQ).

To obtain a preliminary estimate of the Brillouin shift and linewidth, we first fit each Brillouin peak in the $d=10$ mm VV spectra to the damped harmonic oscillator function

$$I(\omega)=\frac{I_0}{\omega}\mathrm{Im}[\omega^2-\omega_B^2-i\omega\gamma_B]^{-1}=\frac{I_0\gamma_B}{[\omega^2-\omega_B^2]^2+[\omega\gamma_B]^2}, \tag{2}$$

including convolution with the instrument function. In Fig. 4 the resulting values of $\omega_B(a)$ and $\gamma_B(b)$ are shown by the points. For a simple liquid, both ω_B and γ_B would have simple monotonic temperature dependence. Theob-

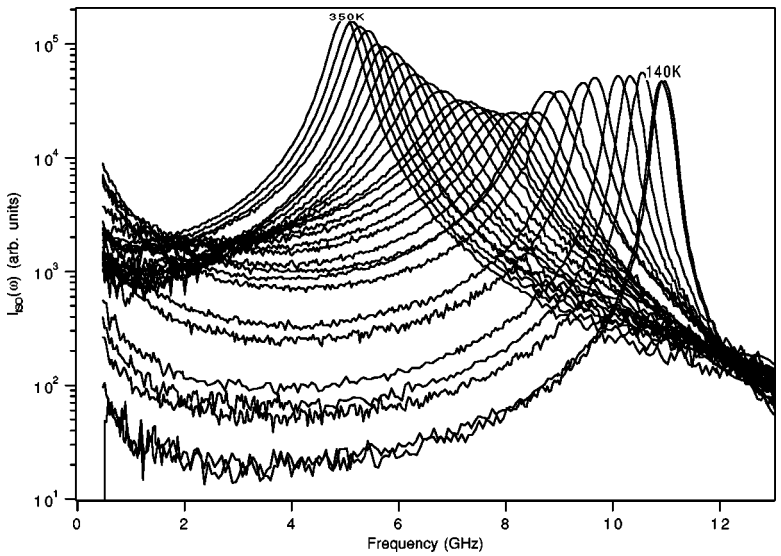

FIG. 3. Complete set of composite $I_{ISO}(\omega)$ spectra for 28 temperatures from 140 K to 350 K obtained with the procedure shown in Fig. 2. T = 140, 150, 160, 165, 170, 180, 185, 195, 200, 205, 210, 215, 220, 225, 230, 235, 240, 250, 260, 270, 280, 290, 300, 310, 320, 330, 340, and 350 K, from right to left.

served temperature dependence of ω_B and γ_B, as noted in the Introduction, is the signature of structural relaxation dynamics as seen in Brillouin scattering. The maximum in γ_B at $T \sim 230$ K indicates that the α peak moves through the Brillouin line at that temperature.

III. DATA ANALYSIS 1: THE COLE-DAVIDSON MODEL

A. The memory function approach

The isotropic Brillouin spectrum $I_{ISO}(\omega)$ is usually attributed to density fluctuations $\rho_q(t)$ where the scattering vector

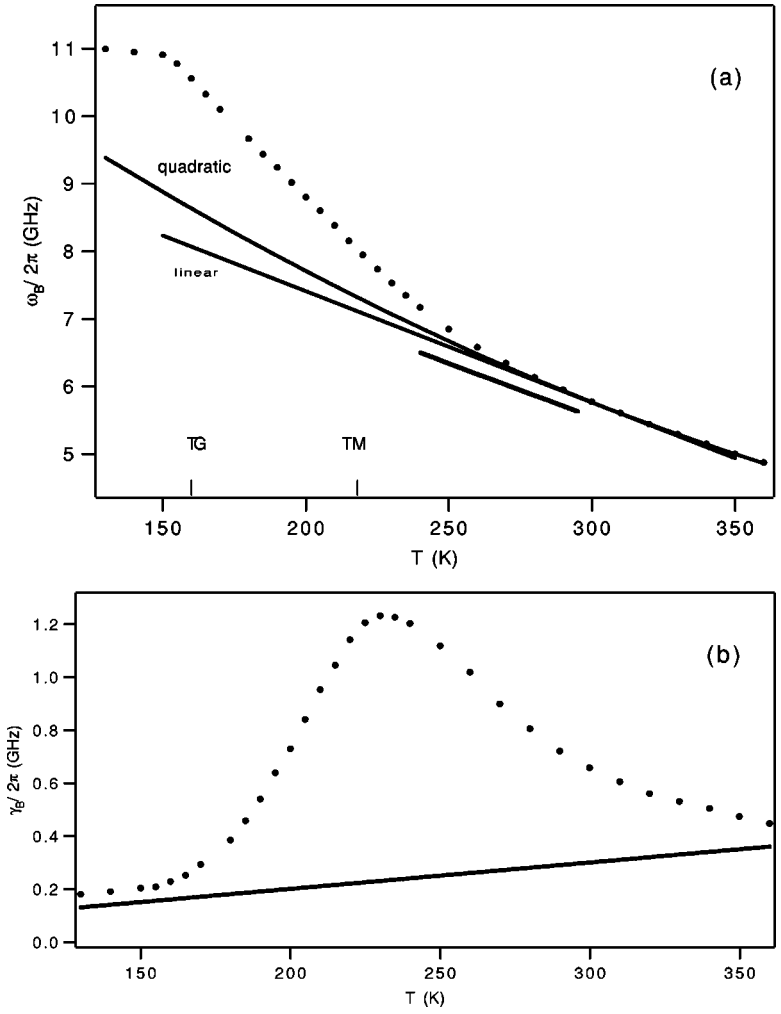

FIG. 4. Fits of the $d = 10$ mm 90° VV Brillouin peaks to Eq. (2) including convolution with the instrument function. (a) $\omega_B/2\pi$ (GHz) (circles). Short solid line: ω_0 from ultrasonic and refractive index data; long solid line: ω_0 increased by 3.5% to match ω_B in the high-temperature region. Solid curved line: quadratic fit $\omega_0(T) = 13.211 - (3.291 \times 10^{-2})T + (2.6973 \times 10^{-5})T^2$. (b) $\gamma_B/2\pi$ (GHz) (circles). Solid line: $\gamma_0 = T/1000$.

$q=(2\pi n/\lambda)\sin(\theta/2)$. The spectrum consists of a triplet: the central thermal diffusion mode (which is generally located at frequencies too low to observe in these experiments and will be ignored in most of the fits) and the Brillouin doublet. The spectrum is conventionally described by

$$I(\omega)=\frac{I_0[\gamma_0+m''(\omega)]}{[\omega^2-\omega_0^2+\omega m'(\omega)]^2+[\omega\gamma_0+\omega m''(\omega)]^2}. \quad (3)$$

[The particular Laplace transform convention used to derive Eq. (3) is discussed in the Appendix.]

Equation (3) is very general; $m(\omega)=m'(\omega)+im''(\omega)$ is the Laplace transform of the memory function $m(t)$, which can be constructed to include structural relaxation, thermal diffusion, and translation-orientation coupling for liquids of anisotropic molecules [20–22]. Usually, however, $m(t)$ represents the relaxing longitudinal viscosity, first introduced by Mountain [1] to describe the damping of sound waves by interaction with the internal degrees of freedom of the molecules, and later utilized to represent the interaction of sound waves with structural relaxation. (Both mechanisms may contribute, however, as discussed below.) In the long-wavelength limit, $\omega_0=C_0q$ where C_0 is the limiting low-frequency adiabatic sound velocity, and γ_0 is the ''regular'' sound attenuation coefficient. Note that Eq. (3) is the power spectrum of a damped harmonic oscillator with a frequency-dependent damping function $\gamma(\omega)=\gamma_0+m''(\omega)$.

Ideally, the $I_{ISO}(\omega)$ spectra should be analyzed to yield $m(\omega)$ directly. But in practice this is not possible because the spectra only cover a range of two decades at most, while $m(\omega)$ extends over many decades. Also, the spectra are dominated by the Brillouin components [which would be the complete spectrum of Eq. (3) if $m(\omega)=0$], and the modification of $I(\omega)$ produced by inclusion of $m(\omega)$ is not very sensitive to the detailed form of $m(\omega)$. Therefore, data analysis almost always proceeds by selecting a parametrized model for $m(\omega)$ and varying the parameters at each temperature to optimize the fits.

The primary requirements on $m(\omega)$ are that $m'(\omega_B)$, the real part of $m(\omega)$ at the frequency of the Brillouin peak, must be adjusted to shift the Brillouin peak from ω_0 to ω_B, and $m''(\omega_B)$, the imaginary part of $m(\omega)$ at the frequency of the Brillouin peak, must be adjusted so that $\gamma_0+m''(\omega_B)$ will give the correct Brillouin linewidth. If these two conditions are simultaneously satisfied, then the particular form chosen for $m(\omega)$ will only influence the details of the line shape. Therefore the essential requirement is that $m''(\omega_B)/m'(\omega_B)$ must have the ''correct'' value. Nevertheless, this is not a trivial requirement since $m'(\omega)$ and $m''(\omega)$ are connected by Kramers-Kronig relations.

The prototype memory function is the exponential $e^{-t/\tau}$, multiplied by a coupling constant Δ^2. (It is usually called Debye relaxation although it was first used by Maxwell in his theory of viscoelasticity.) The simplest memory function $m(t)$ for structural relaxation that fits various experimental data in the frequency region of α relaxation is the stretched-exponential Kohlrausch-Williams-Watts (KWW) function $e^{-(t/\tau)^{\beta_K}}$. An approximation to the Fourier transform of this $m(t)$ is provided by the Cole-Davidson (CD) function

$$m(\omega)=(\Delta^2/\omega)[(1-i\omega\tau)^{-\beta}-1], \quad (4)$$

which has frequently been used, together with Eq. (3), to analyze Brillouin-scattering spectra. In practice, the fitting procedure adjusts the coupling constant Δ^2 so that the real part of $m(\omega)$ produces the correct ω_B for the Brillouin peak, while τ is adjusted to give the correct Brillouin linewidth.

There are several problems that should be noted in carrying out this analysis, as well as analyses with more elaborate memory functions.

(1) Many glass-forming materials are molecular liquids, and internal vibrational modes may also contribute to $m(\omega)$, as originally proposed by Mountain [1]. Recently, Monaco *et al.* [5] have carried out a Brillouin-scattering study of OTP from which they conclude, for OTP, that the fast part of the relaxation process is *entirely* due to intramolecular vibrational modes. The assignment results from the presence of additional low-frequency structures (Mountain mode) in VV, but not VH, spectra, in both the glass and the crystal. This conclusion has recently found additional support from a molecular dynamics study of OTP [23]. There is no evidence, however, that it applies to other materials such as PC, and it will not be considered here.

(2) The identification of $I_{ISO}(\omega)$ with density fluctuation rests on the assumption that scattering due to orientational fluctuations, which is typical for molecular glass-forming materials, is eliminated by the subtraction of $I_{ani}(\omega)$ from $I_{VV}(\omega)$ described in the preceding section. However, two consequences of anisotropy may remain after subtraction. First, since longitudinal current involves both compression and shear, rotation-translation coupling modifies the longitudinal current correlator [which determines the spectrum of $\rho_q(t)$] as shown in Eq. (A.14) of Ref. [24]. Second, as noted recently by Latz and Letz and by Franosch *et al.* [25], because of this coupling the orientational dynamics also reflect the longitudinal acoustic mode, and this part of the orientational dynamics is not removed by subtraction. Therefore, both density fluctuations and orientational dynamics may contribute to the $I_{ISO}(\omega)$ spectra.

While the extent of these corrections due to molecular anisotropy is not yet clear, preliminary simulations, carried out in collaboration with Pick, indicate that they are relatively minor. We will, therefore, use the conventional memory function formalism in this paper, recognizing that the values of the parameters used to describe the frequency-dependent longitudinal viscosity may reflect some aspects of translation-rotation coupling and molecular anisotropy and may also include some contribution from intramolecular vibrational dynamics.

B. Cole-Davidson fits

We first analyzed the $I_{ISO}(\omega)$ spectra of Fig. 3 using Eq. (3) with the CD memory function $m(\omega)$ of Eq. (4). The fit results, for a subset of the spectra, are shown in Fig. 5 [26].

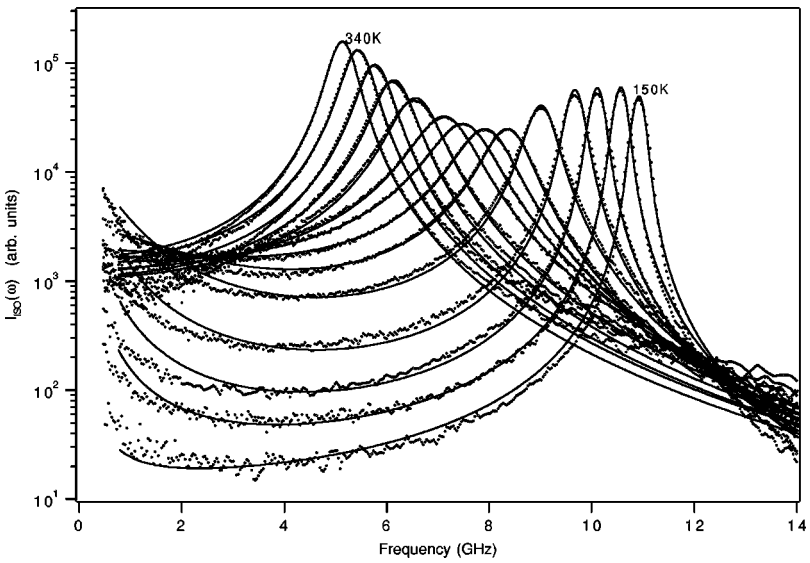

FIG. 5. Cole-Davidson fits to the $I_{ISO}(\omega)$ spectra of Fig. 3 to Eqs. (3) and (4), with $\beta=0.68$, $\omega_0/2\pi=13.211-(3.291\times10^{-2})T+(2.6973\times10^{-5})T^2$, $\gamma_0/2\pi=T/1000$. The fits are shown for $T=150$, 160, 170, 180, 195, 210, 220, 230, 240, 260, 280, 300, 320, and 340 K.

As often found in the past, excellent fits can be obtained if all the parameters are kept free. However, it is preferable to fix as many parameters as possible using independently determined values, since the parameters are rather strongly coupled. (This coupling can also lead to unstable parameter values in the fit results.) Here we consider each of the relevant parameters separately.

(1) β. The fits are relatively insensitive to this parameter. We took $\beta=0.68$ (corresponding to $\beta_K=0.77$) as found in the analysis of depolarized backscattering spectra by Du *et al.* [8].

(2) $\omega_0(T)$. Since $\omega_0=C_0q$, where C_0 is the limiting low-frequency adiabatic sound velocity and q is the scattering wavevector $(4\pi n/\lambda)\sin(\theta/2)$, $\omega_0(T)$ can be fixed if $C_0(T)$ and the refractive index $n(T)$ are known. $C_0(T)$ was previously measured by ultrasonic experiments at 5 MHz and 15 MHz by Du *et al.* [8], which gave $C_0(T)=2.507\times10^5-361.2T$ cm/sec. However, the ultrasonic data only cover the range 240–293 K. At lower temperatures, there is significant dispersion in the ultrasonic sound speed, while higher-temperature measurements are technically difficult. The refractive index $n(T)=1.5314-(3.752\times10^{-4})T$ (see Table I) corresponds to the sodium D line and may be different at 514.5 nm. The $\omega_0(T)$ values implied by these measurements are shown in the upper panel of Fig. 4, by the short solid line. A linear extrapolation of these values, shifted up by 3.5%, is indicated by the long solid line labeled "linear:" $\omega_0(T)/2\pi=(10.71-0.0165T)$ GHz. The shift, which is within the experimental errors of the $C_0(T)$ and $n(T)$ data, was chosen so that at high temperatures the Brillouin peak frequency ω_B is equal to ω_0, as expected. Note, however, that the high-T ω_B values suggest some small upward curvature away from the linear extrapolation above 320 K.

Initially, fits were carried out with this linear-T estimate of $\omega_0(T)$. However, the fits were not all satisfactory, in part because of the high-T curvature in ω_B seen in Fig. 4. For materials where $C_0(T)$ measurements extend over larger temperature ranges, there can be a significant upward curvature to $C_0(T)$. We, therefore, tried fitting $\omega_0(T)$ to the six highest-temperature $\omega_B(T)$ values plus one $\omega_0(T)$ value obtained from a free CD fit at 230 K where the Brillouin linewidth is largest. The result was the quadratic $\omega_0(T)$ function shown by the upper solid line in Fig. 4 labeled "quadratic,"

$$\omega_0(T)=13.211-(3.291\times10^{-2})T+(2.6973\times10^{-5})T^2, \tag{5}$$

which was used in all subsequent fits.

(3) $\gamma_0(T)$. This term is conventionally included to represent "regular" damping of the sound waves by anharmonic processes not related to structural relaxation. It can also represent a simple frequency-independent approximation for the fast part of the structural relaxation not included in α-relaxation-only models such as the CD function. Usually, γ_0 is taken as a temperature-independent constant, fixed from the Brillouin linewidth at low temperatures. However, since anharmonic damping processes often tend to become stronger with increasing temperature, γ_0 may increase with T. Also, at temperatures well above the temperature of the maximum Brillouin linewidth, the linewidth due to γ_0 plus structural relaxation is approximately given by $\Delta\omega_B\approx\gamma_0+\Delta^2\tau\beta$. Fits with constant γ_0 often give Δ^2 values that increase at high temperatures, a result that appears to be unphysical. This apparent increase in Δ^2 can be avoided by allowing γ_0 to increase with increasing T. To avoid introducing additional fitting parameters we arbitrarily assumed γ_0 to be a linear function of T, and took $\gamma_0(T)=T/1000$ as shown by the solid line in the lower panel of Fig. 4.

(4) $\Delta^2(T)$. Since at high temperatures $\omega_B=\omega_0$ while $\Delta\omega_B=\gamma_0+\Delta^2\tau\beta$, the effective fitting parameter for $\Delta\omega_B$ at high temperatures is the product $\Delta^2\tau$. So if Δ^2 and τ are both free parameters, the fits tend to be unstable. We, therefore, carried out the fits for temperatures up to 235 K with the three free fitting parameters: Δ^2, τ, and the scale factor I_0. For $T>235$ K, Δ^2 was fixed at its value at ~235 K, and the fits were carried out with only τ and I_0 free. The parameters $\tau(T)$ and $\Delta^2(T)$ obtained from these fits are shown in Table II along with the reduced χ^2 value for each fit. The CD

TABLE II. Parameters obtained from the fits

				Hybrid (fixed τ)					Schematic MCT			
T(K)	CD (free τ)				$\beta=0.68$		$\beta=b=0.5$		τ (ns)	V_s^{DLS}	V_s^{BR}	χ^2
	τ (ns)	Δ^2 (GHz^2)	χ^2	τ (ns)	B/Δ^2	χ^2	B/Δ^2	χ^2				
140	790	36.5	27.2	1.26×10^{22}								
150	1220	40.2	27.8	1.42×10^{14}	0.01	27.4	0.002	28.6		94		
160	31.8	37.0	22.1	2.49×10^{8}	0.04	19.5	0.034	22.7		80	30	25.2
165	14.2	34.3	23.3	1.96×10^{6}								
170	6.11	31.8	41.3	4.28×10^{4}	0.11	12.5	0.13	15.9		60		
180	1.34	27.5	66.3	2.11×10^{2}	0.53	8.4	0.32	20.3	2.9×10^{1}	50	13	31.4
185	0.763	25.3	84.6	3.40×10^{1}								
195	0.236	22.0	60.4	2.51	1.50	47.3						
200	0.148	20.6	44.2	9.75×10^{1}		35.2	1.31	23.3	2.4×10^{-1}	30	7.6	5.85
205	1.03×10^{-1}	19.5	28.8	4.47×10^{-1}								
210	7.28×10^{-2}	18.4	16.4	2.33×10^{-1}	4.00	10.1	2.72	8.3		25		
215	5.41×10^{-2}	17.6	17.8	1.34×10^{-1}								
220	4.15×10^{-2}	17.0	8.99	8.35×10^{-2}		19.2	18.1	5.75	3.0×10^{-2}	23	5.4	5.73
225	3.25×10^{-2}	16.9	9.43	5.55×10^{-2}	4.00	19.5						
230	2.53×10^{-2}	16.7	5.21	3.89×10^{-2}		20.3	36.0	12.1		21		
235	2.13×10^{-2}	17.0	5.35	2.85×10^{-2}								
240	1.75×10^{-2}	17.0	11.9	2.16×10^{-2}	4.00	14.2	24.8	13.2	9.9×10^{-3}	18	4.7	11.9
250	1.28×10^{-2}	17.0	25.7	1.36×10^{-2}						16		
260	9.96×10^{-3}	17.0	50.0	9.29×10^{-3}	4.00	41.6	21.2	41.3	4.7×10^{-3}	15	4.3	39.9
270	8.17×10^{-3}	17.0	47.4	6.80×10^{-3}						13		
280	6.61×10^{-3}	17.0	66.3	5.24×10^{-3}	4.00	54.3	22.0	54.0		12	<3.5	51.9
290	5.58×10^{-3}	17.0	60.5	4.19×10^{-3}								
300	4.57×10^{-3}	17.0	60.7	3.46×10^{-3}	4.00	53.5	0.87	53.5			<2.5	
310	3.90×10^{-3}	17.0	43.4	2.93×10^{-3}								
320	3.38×10^{-3}	17.0	49.2	2.53×10^{-3}	4.00	44.3	2.34	44.3			<2.5	40.5
330	2.76×10^{-3}	17.0	38.1	2.22×10^{-3}								
340	2.26×10^{-3}	17.0	26.3	1.98×10^{-3}								
350	1.80×10^{-3}	17.0	18.2	1.79×10^{-3}	4.00	18.1	1.90	18.1			<2.5	18

fits, shown in Fig. 5, are satisfactory although better fits could be obtained by keeping more parameters free, especially ω_0.

However, the major point of the CD fits, as shown by the solid circles in Fig. 1, is that for temperatures below $\sim$230 K, τ_α^{CD} determined from these fits does not increase very rapidly with decreasing T. At $T=T_G=160$ K, τ_α^{CD} found from the CD fits is only $\sim$30 ns, compared to τ $\sim$100 s found in other experiments. This disagreement is generally recognized as indicating that the CD model (or any α-relaxation-only model) for $m(\omega)$ is incomplete. Once the α peak moves well below the frequency of the Brillouin peak, $m''(\omega)$ of the CD function [with reasonable $\tau(T)$ values] decreases rapidly with decreasing temperature, while the shape of the spectrum indicates that a significant contribution from $m''(\omega)$ is still present in the region of the Brillouin peak.

The fact that the CD function is an incomplete representation of the structural relaxation dynamics can also be seen directly in the PC dielectric data of Schneider *et al.* [18]. Their Fig. 2 shows CD fits to the dielectric data, which are excellent for the α peak, but which fall below the experimental data in the high-frequency wing.

IV. DATA ANALYSIS 2: INCLUDING THE FAST β RELAXATION—THE HYBRID MODEL

The $\tau(T)$ values obtained from the Cole-Davidson fits to Brillouin spectra exhibit a temperature dependence at low temperatures that disagrees strongly with the results of other experiments, as seen in Fig. 1. The origin of this apparent disagreement can be attributed to the use of ''α-relaxation only'' models for $m(t)$, which ignore the fast part of the relaxation process preceding the final α relaxation (i.e., the β relaxation in mode-coupling theory). The need for an ''additional fast contribution'' to $m(\omega)$ was first noted by Loheider *et al.* [2] (also see [3]). Several empirical approaches to extending $m(\omega)$ or $m(t)$ to include the missing fast β relaxation have been described in the literature, including (1) adding a second Debye, Cole-Cole, or Cole-Davidson function to the Cole-Davidson α-relaxation term [4–6], (2) extracting a memory function including both α and β relaxation from

depolarized backscattering spectra and using it for fitting the Brillouin spectra [3] (a procedure that succeeded for calcium potassium nitrate (CKN) but not for other materials), (3) taking $m(t)$ as the sum of a stretched exponential plus a damped high-frequency oscillatory term [7], and (4) adding a term $B\omega^a$ to the Cole-Davidson function to approximate the critical-decay component of the fast β relaxation predicted by the MCT [8,9,3,10]. This additive ''hybrid model'' approach, initially suggested by Götze [27], has recently been shown to provide excellent fits to depolarized backscattering spectra of toluene [28] and has also been used in the analysis of Brillouin spectra of metatoluidine [10].

With approach (1) the additional fast CD or Lorentzian, with relaxation time $\tau_\beta \sim 30$ ps, is able to explain the extra ''Mountain mode'' seen in OTP at low temperatures [29]. We note that attributing a fast relaxation time τ_β to structural relaxation is incompatible with MCT, which describes the fast relaxation by power laws in ω or t for which there is no τ_β [30], although it may represent an intramolecular relaxation process.

A. The hybrid model

We have utilized the hybrid model approach, which has been employed in several previous Brillouin-scattering studies. We begin with the CD function [Eq. (4)] and add a term to $m(\omega)$ proportional to ω^{a-1}, which represents the t^{-a} ''critical-decay'' part of the fast β process in MCT. This superposition approximates the two-step relaxation scenario of MCT and does not introduce another relaxation time τ_β.

In some previous studies, we have used a related procedure to analyze depolarized backscattering spectra. For orthoterphenyl, we combined extended MCT fits for the β-relaxation region with KWW fits for the α peak [31]. A comparison of these two hybrid procedures has not yet been attempted.

Two problems arise when the term t^{-a} is added to $m(t)$. First, the resulting ω^a term in $\omega m(\omega)$ extends to arbitrarily high frequencies rather than terminating in the boson peak. This is presumably unimportant for Brillouin scattering, however, since fits to the Brillouin spectra are limited to $\omega/2\pi \lesssim 15$ GHz. Second, $m''(\omega)$, which appears in the numerator of $I(\omega)$ in Eq. (2), diverges at low frequencies as ω^{a-1} resulting in the introduction of a spurious ''central peak.'' To eliminate this artifact, we have included an exponential cutoff in the critical decay part of $m(t)$ [27],

$$m_{crit}(t) = Bt^{-a}e^{-(t/\tau)}, \tag{6}$$

where τ is the same τ_α^{CD} of the CD function, Eq. (4). (Note that this cutoff factor has not been included in previous analyses based on the hybrid model.)

With this modification, the hybrid memory function becomes

$$\omega m(\omega) = \Delta^2[(1-i\omega\tau)^{-\beta}-1] + i\omega B\Gamma(1-a)(\tau^{-1}-i\omega)^{a-1}. \tag{7}$$

[See the Appendix for the derivation of Eq. (7).]

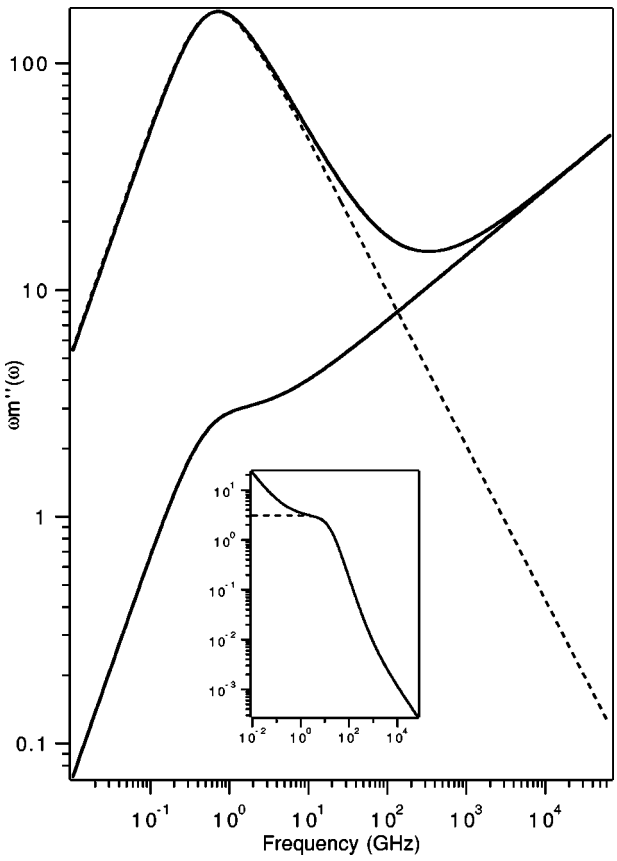

FIG. 6. The hybrid memory function $\omega m''(\omega)$ of Eq. (7) with $\tau = 0.3$ ns, $\beta = 0.68$, and $a = 0.29$. The broken line is the CD function and the lower solid line is the critical-decay term. The ratio of the critical decay to CD contributions is $B/\Delta^2 = 0.005$. Inset: $m''(\omega)$ vs ω for the hybrid model [Eq. (7)] with $\tau = 0.01$ ns, $\Delta = 20$ GHz, and $B = 5$ without a cutoff (upper line), and with the cutoff $e^{-t/\tau}$ in Eq. (6) (lower line), illustrating how the cutoff eliminates the spurious central peak.

At high frequencies where $\omega\tau \gg 1$, the critical decay part of Eq. (7) becomes

$$\omega m_{CR}(\omega) = [B_1 + iB_2]\omega^a \tag{8}$$

(where $B_1 = B\sin[\pi(a-1)/2]\Gamma(1-a)$ and $B_2 = B\cos[\pi(a-1)/2]\Gamma(1-a)$). Equation (8) is the familiar high-frequency power-law behavior predicted by MCT.

In Fig. 6 we plot $\omega m''(\omega)$ of Eq. (7) with $\tau = 0.3$ ns, $\beta = 0.68$, and $a = 0.29$. The broken line is the Cole-Davidson term only, and the lower solid curve is the critical-decay term only, including the exponential cutoff. The upper solid curve is the full hybrid memory function $\omega m''(\omega)$ of Eq. (7) with $B/\Delta^2 = 0.005$. This figure illustrates how the resulting $\omega m''(\omega)$ goes over smoothly from the CD α-peak behavior at low frequencies to the ω^a behavior at high frequencies, with a minimum between the two regions. The inset of Fig. 6 shows the full $m''(\omega)$ with and without the $e^{-t/\tau}$ cutoff, illustrating how the spurious central peak is eliminated by the exponential cutoff.

B. The critical exponent *a*

In MCT, the function $\omega m''(\omega)$ is predicted to have a minimum between the high-frequency von Schweidler wing of the α peak and the critical-decay region similar to that in Fig. 6. In the region of this minimum, the MCT interpolation approximation gives $\omega m''(\omega)$ in terms of the critical exponents a and b (which are connected by the Γ function relation) by [30]

$$\omega m''(\omega) = \omega m''_{min}(\omega)[b(\omega/\omega_{min})^a + a(\omega_{min}/\omega)^b]/(a+b), \tag{9}$$

where a is the critical exponent and b is the von Schweidler exponent, representing the high-frequency wing of the α peak. For $a=0.29$, MCT predicts $b=0.50$.

Since in our hybrid memory function, Eq. (7), the CD function for $\omega\tau \gg 1$ is $\propto \omega^{-\beta}$, fits to the interpolation Eq. (9) with $b=\beta$ will determine an ''effective'' a_{eff} to use in Eq. (7) at temperatures high enough for the minimum to be observable (from previous MCT fits, $b \approx 0.50$ while $\beta \sim 0.68$). At lower T, where the minimum has disappeared from the frequency region of the Brillouin spectrum, $\omega m''(\omega)$ may have the form of a power law in ω, but since this region no longer corresponds to the asymptotic region of the minimum, the apparent power-law behavior of $\omega m''(\omega) \propto \omega^{a_{eff}}$ can produce an a_{eff} quite different from the critical exponent a itself.

We utilized the depolarized backscattering spectra $I_{VH}(\omega)$, multiplied by ω to estimate $\omega m''(\omega)$ in order to find $a_{eff}(T)$. In Fig. 7 we show six $\omega I_{VH}(\omega)$ spectra for $T=140$, 150, 160, 170, 180, and 185 K. The spectra for $T=170$, 180, and 185 K, where the minimum is visible, have been fit to the interpolation equation [Eq. (9)] using $\beta=0.68$ for b with a free, while the spectra for $T=140$, 150, and 160 K have been fit to $\omega^{a_{eff}}$. The values of $a_{eff}(T)$ found from these fits are

T (K)	a_{eff}
140	0.62
150	0.59
160	0.52
170	0.42
180	0.30

In the fits to our Brillouin spectra, we used these values of $a_{eff}(T)$ for temperatures up to 180 K and $a=0.29$ for all higher temperatures. (Note that the temperatures at which a_{eff} differs from $a=0.29$ are all below T_C.)

A tendency for a_{eff} to increase with decreasing T at low temperatures has been found previously in depolarized light-scattering studies of several glass-forming materials, including CKN, OTP, PS, PC, and picoline [32]. As we will see, the fits to our Brillouin-scattering spectra suggest that this increase also applies to the memory function for the longitudinal viscosity.

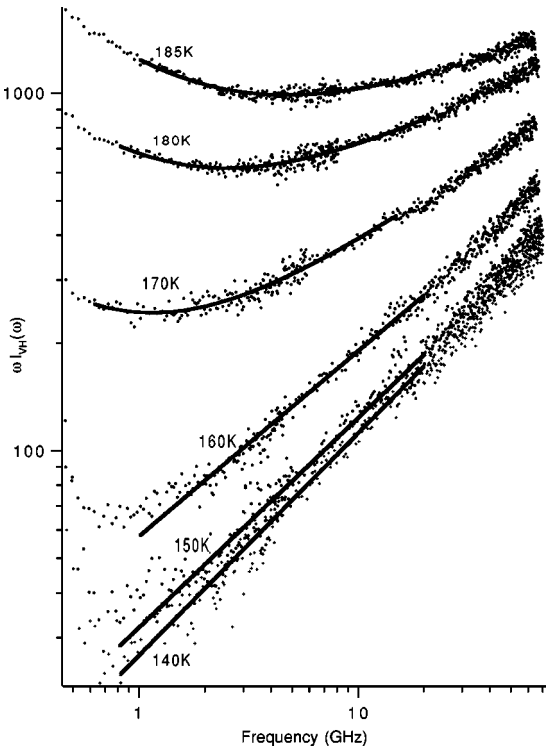

FIG. 7. VH backscattering spectra multiplied by frequency with fits to the MCT interpolation equation [Eq. (9)] (using $b=\beta=0.68$ and a free) ($T=170$, 180, 185 K) or the power law $\omega^{a_{eff}}$ ($T=140$, 150, 160 K). The values of a_{eff} determined in these fits were used in the low-temperature $I_{ISO}(\omega)$ hybrid model fits shown in Figs. 8 and 9.

C. Minimum free parameter analysis

We initially tried to fit the spectra with Eq. (3) and the hybrid memory function Eq. (7) with the smallest possible number of free parameters. We fixed $\omega_0(T)$ with Eq. (5), $\gamma_0(T)=T/1000$ as in the Cole-Davidson fits, τ using Eq. (1), $\beta=0.68$, and the ratio B/Δ^2, the relative strengths of the critical-decay term (B) and Cole-Davidson term (Δ^2), by adjusting B/Δ^2 to make ω_{min} fall close to the ω_{min} found in the depolarized backscattering PC $\chi''(\omega)$ spectra of Du *et al.* [8]. With $B/\Delta^2=0.175$, which produced good agreement, there are only two remaining free parameters left in Eqs. (7) and (3): the CD coupling constant Δ^2 and the overall normalization constant I_0.

With this severely constrained fit procedure, however, the resulting fits were not generally acceptable. One surprising aspect of the results was that for $T \leqslant 170$ K the linewidths of the fits became too broad; this problem can be resolved by *decreasing* B/Δ^2.

This indication that the strength of the critical contribution to the memory function (relative to the α peak) may weaken in the temperature range between T_C and T_G is also supported by the depolarized backscattering spectra, shown in Fig. 7. At temperatures below $T=170$ K, the minimum in $\omega I(\omega)$ is at $\omega \leqslant 1$ GHz, so the α peak is completely out of the spectral window. The intensity in the Brillouin frequency region (~ 8 GHz), which is, therefore, entirely due to the ''fast beta decay,'' is seen to decrease rapidly with decreasing

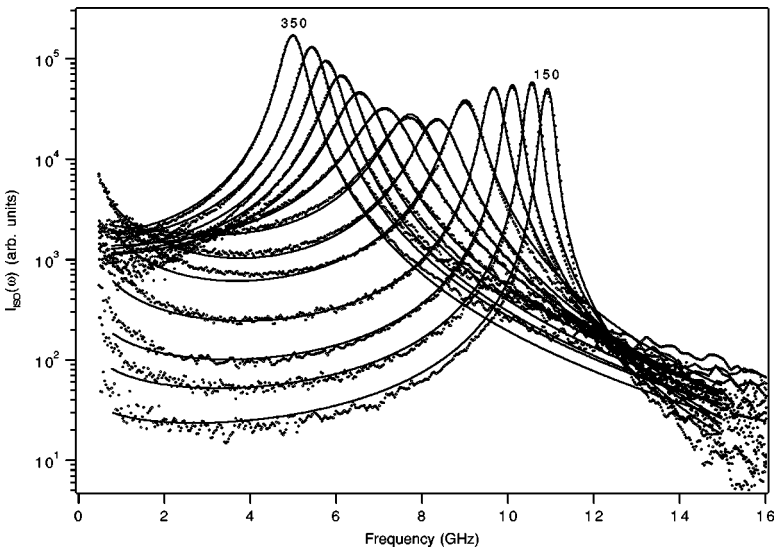

FIG. 8. Fits to PC Brillouin spectra $I_{ISO}(\omega)$ with the hybrid model for $m(\omega)$ of Eq. (7) with $\beta=0.68$. The free fitting parameters are I_0, Δ^2, and B/Δ^2; the values found from the fits are given in Table II. $T=150$, 160, 170, 180, 195, 210, 225, 240, 260, 280, 300, 320, and 350 K.

T, consistent with the apparent behavior of $\omega m(\omega)$. This result is also presumably related to the MCT prediction of a cusp in the nonergodicity parameter $f_q(T)$ at T_C below which the critical decay weakens with decreasing temperature. It also indicates that additional contributions to the fast relaxation from other processes (e.g., intramolecular vibrations) are unlikely in PC since these would produce a larger value of B/Δ^2.

D. Complete hybrid model fits

To provide a complete hybrid model analysis, we allowed the ratio B/Δ^2 to vary in the fit. At low temperatures, B and Δ^2 could be determined independently from the fit. At temperatures above 200 K, however, B and Δ^2 are strongly correlated. At 210 K an optimum fit was found with $B/\Delta^2=4.0$, and we arbitrarily kept this value fixed for all temperatures above 210 K. For $T<180$ K, the fits obtained with $a=0.29$ were not satisfactory, so they were redone with the a_{eff} values listed above. The resulting set of fits is shown in Fig. 8; the fitting parameters B/Δ^2 and τ are given in Table II together with the χ^2 values. These hybrid model fits have three free parameters, as in the CD fits. However, they have $\tau(T)$ constrained to follow Eq. (1) shown by the broken line in Fig. 1, automatically eliminating the $\tau(T)$ disagreement problem of the CD fits. They are nevertheless at least as good as the CD fits.

In their light scattering study of metatoluidine, Aouadi *et al.* [10] also analyzed $I_{ISO}(\omega)$ spectra with the hybrid model, constraining τ_α^{CD} to be proportional to the τ_α determined from depolarized backscattering spectra. They found, as we did, that at low temperatures the strength of the critical decay decreases with decreasing T (see their Fig. 12). Although they also found that the critical-decay strength decreases at high temperatures, resulting in an apparent maximum around 250 K, this behavior may be a manifestation of the strong correlation between Δ^2 and B mentioned above.

E. Thermal diffusion contribution

With a_{eff} replacing a in Eq. (7), we carried out additional fits to the Brillouin spectra for $T=150$, 160, 170, and 180 K. The fits are shown by the lower curves for each temperature in Fig. 9. (They are also the four low-T fits shown in Fig. 8.) Note that at low temperatures the experimental spectra have a weak extra structure at low frequencies, which is not present in the theoretical fits.

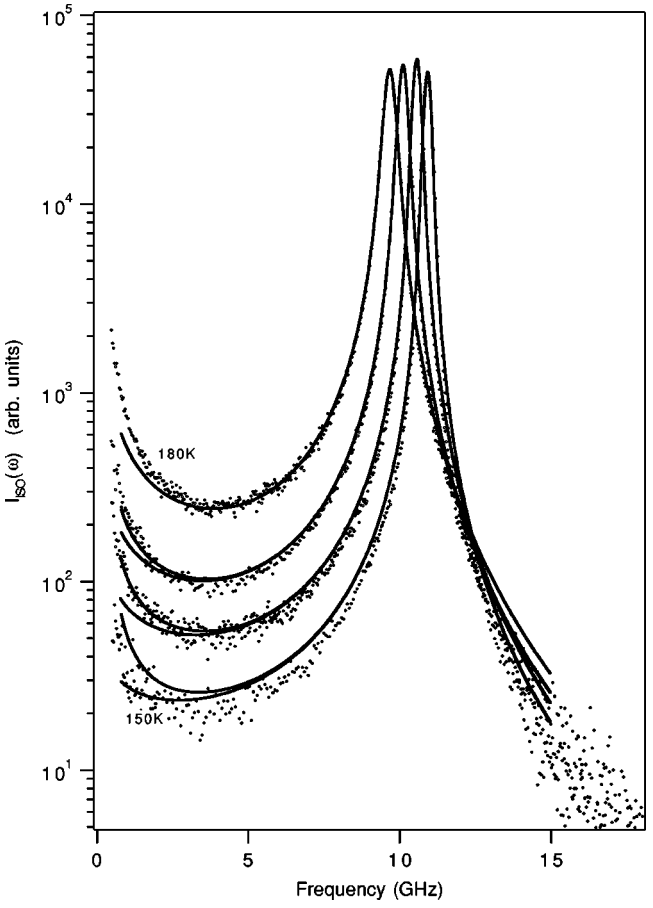

FIG. 9. Low-temperature hybrid model fits using the a_{eff} values found in the fits shown in Fig. 7. For $T=150$, 160, and 170 K, a second fit (the upper curve at each temperature) is shown for each spectrum, which includes the effect of thermal diffusion.

The light-scattering spectrum of density fluctuations $I_{ISO}(\omega)$, including thermal diffusion effects, can be expressed as [21,22]

$$I(\omega)=\frac{I_0}{\omega}\mathrm{Im}[\omega_T^2-\omega^2-i\omega\gamma_0-\omega m(\omega)]^{-1}, \qquad (10)$$

where $\omega_T=C_Tq$ (C_T is the isothermal sound velocity) and $m(\omega)=m_\eta(\omega)+m_{Th}(\omega)$ includes both the structural relaxation contribution $m_\eta(\omega)$ [e.g., Eq. (4) or (7)] and the thermal diffusion contribution

$$m_{Th}(t)=(\gamma-1)\omega_T^2e^{-t/\tau_{Th}},$$

where $\tau_{Th}=(D_Tq^2)^{-1}$. With the Laplace transform convention of Eq. (A3) in the Appendix,

$$m_{Th}(\omega)=\frac{i(\gamma-1)\omega_0^2\tau_{Th}}{1-i\omega\tau_{Th}}. \qquad (11)$$

In the spectral window explored by 90° Brillouin scattering ($\omega\gtrsim0.5$ GHz), $\omega\tau_{Th}\gg1$ since typically $\tau_{Th}\sim15$ ns. Then, in Eq. (10), $-\omega m_{Th}(\omega)\sim\omega_T^2(\gamma-1)$. Adding this to the ω_T^2 term in Eq. (10) then gives $\omega_T^2+\omega_T^2(\gamma-1)=\omega_T^2\gamma$, which is just the square of the adiabatic sound frequency ω_0. In that approximation Eq. (10) recovers the simpler equation [Eq. (3)] with $m(\omega)\equiv m_\eta(\omega)$ only.

While the quasielastic thermal diffusion mode is not usually included in the analysis of Brillouin-scattering spectra, at low temperatures, the high-frequency tail of the thermal diffusion mode can appear in the Brillouin spectrum if the window extends to sufficiently low frequencies. The four spectra shown in Fig. 9 have a weak extra structure at low frequencies, which may be due to the tail of the thermal diffusion mode.

Since numerical data for γ and D_T are not available for PC (to our knowledge), we estimated $\gamma=1.5$ and $\tau_{Th}=16$ ns, and reanalyzed the spectra of Fig. 9 using Eq. (10) with $\omega_T^2=\gamma\omega_0^2$, $m(\omega)=m_\eta(\omega)+m_{Th}(\omega)$ with $m_{Th}(\omega)$ given by Eq. (11), and $m_\eta(\omega)$ by Eq. (7). The resulting fits, including thermal diffusion, are shown as the upper curves for each temperature in Fig. 9 for $T=150$, 160, and 170 K, showing that at these low temperatures, the thermal diffusion mode is apparently visible in the Brillouin spectrum at low frequencies. For temperatures above 170 K, the thermal diffusion contribution is not visible.

F. Hybrid model with $\beta=b$

Finally, we note that a slightly different strategy can be followed in carrying out the hybrid model analysis. With the exponent a in Eqs. (6) and (7) fixed (for $T>T_C$) at 0.29, the region of the minimum in $\omega m''(\omega)$ is predicted by MCT to obey Eq. (9) with $b=0.50$. However, there is a slight difference between this prediction and Eq. (7) because so far we have taken $\beta\neq b$. This difference can be eliminated by arbitrarily fixing $\beta=b=0.50$, as was done for the analysis of depolarized backscattering spectra of toulene by Wiedersich *et al.* and of picoline by Adichtchev *et al.* [28], which reduced the number of free fitting parameters in their fits by one.

We, therefore, carried out another set of hybrid model fits with $\beta=b=0.5$. All other parameters were the same as in the fits of Fig. 8. In these fits, we kept $a=0.29$ and $\beta=0.50$ for all temperatures and also kept both Δ^2 and B free. The resulting fits are generally comparable to those obtained with $\beta=0.68$, demonstrating that the hybrid model fits are not very sensitive to the value of β.

At low temperatures, however, the low-frequency regions of these fits are not as good as the previous fits, illustrating the effect of the increase in a_{eff} at low T. The χ^2 values obtained both with $\beta=0.68$ and $\beta=0.5$ are listed in Table II together with the B/Δ^2 values, and are seen to be similar. Note that in the $\beta=0.5$ fits where Δ^2 and B were both free fitting parameters, B/Δ^2 increases with increasing T, passes through a maximum at $T\sim230$ K, and then decreases again at high T, similar to the results of Aouadi *et al.* for metatoluidine [10]. As noted above, however, B and Δ^2 are strongly correlated at high temperatures, and the high-T values of B/Δ^2 are, therefore, probably not significant.

An advantage of choosing $\beta=b$ is that there is one less parameter in the fitting procedure. Also, the region of the susceptibility minimum in Eq. (9) is the same as in Eq. (7) if $\beta=b$. This makes the $\beta=b$ reduced hybrid model a good candidate for attempting to simultaneously describe all relaxing properties in a given material.

V. DATA ANALYSIS 3: EXTENDED SCHEMATIC MCT MODEL

For the third and final analysis of the PC Brillouin spectra $I_{ISO}(\omega)$, we constructed the memory function $m(\omega)$ of Eq. (3) from the mode-coupling theory rather than from parametrized empirical models, using the extended schematic MCT model of Götze and Voigtmann mentioned in the Introduction [15].

A. Mode-coupling theory

The mode-coupling theory begins with exact classical equations of motion (the generalized Langevin equation) for $\phi_q(t)$, the normalized autocorrelation functions of the density fluctuations $\rho_q(t)$, derived from the Hamiltonian with the Zwanzig-Mori projection-operator formalism [30],

$$\ddot{\phi}_q(t)+\nu\dot{\phi}_q(t)+\Omega_q^2\phi_q(t)+\Omega_q^2\int_0^t m_q(t-t')\dot{\phi}_q(t')dt'=0. \qquad (12)$$

Equation (12) is equivalent to the generalized hydrodynamics equation (3), as shown in the Appendix, but its parameters are determined by the Hamiltonian in the Zwanzig-Mori formalism. In particular, $m_q(t-t')$, which is an empirical memory function in Eq. (3), is the autocorrelation function of the random forces in Eq. (12). A central accomplishment of MCT was the derivation of a closed mode-coupling approximation for $m_q(t)$ as

$$m_q(t)=\sum_{q_1} V(q,q_1,q-q_1)\phi_{q_1}(t)\phi_{q-q_1}(t), \qquad (13)$$

in which the coupling coefficients $V(q,q_1,q-q_1)$ are expressed in terms of the static structure factors S_q, S_{q_1}, and S_{q-q_1}. If the intermolecular potential is known, Eqs. (12) and (13) can be solved self-consistently to find the density correlation functions and spectra [12]. (For liquids of anisotropic molecules, the analysis is further complicated by orientational effects.)

In cases where the intermolecular potential is not known, simplified ''schematic'' MCT models can be used, which include only a few correlators, with the remaining coupling constants considered as fitting parameters. The Sjögren model is a two-correlator schematic model. The ''system'' is represented by the system correlator $\phi(t)$, while the variable being probed experimentally is represented by the probe correlator $\phi_s(t)$. The two memory functions are

$$m(t)=v_1\phi(t)+v_2\phi^2(t), \qquad (14a)$$

$$m_s(t)=V_s\phi(t)\phi_s(t). \qquad (14b)$$

Equation (12), written separately for $\phi(t)$ and $\phi_s(t)$ with the memory function of Eqs. (14), can then be solved self-consistently with v_1, v_2, and V_s as fitting parameters (see Ref. [13]).

For temperatures near and below T_C of MCT, the ''cage effect'' dynamics embodied in Eq. (12) lead to the (usually) unphysical result of total structural arrest. In most glass-forming materials, this arrest is avoided by activated hopping processes, which are included in the extended version of MCT (to a first approximation) via a temperature-dependent hopping parameter Δ. Equation (12) is replaced by [15]

$$\ddot{\phi}(t)+(\Delta+\nu)\dot{\phi}(t)+(\Omega^2+\Delta\nu)\phi(t) + \Omega^2\int_0^t m(t-t')[\dot{\phi}(t')+\Delta\phi(t')]dt'=0. \qquad (15)$$

[Note that the hopping parameter Δ in Eq. (15) is not related to the coupling constant Δ^2 of the Brillouin fits in, e.g., Eq. (7).]

The extended Sjögren model of Götze and Voigtmann consists of two sets of Eq. (15), one for ϕ and one for ϕ_s, with the two memory functions of Eqs. (14). These are to be solved self-consistently.

The parameters of $\phi(t)$ are Ω, ν, Δ, v_1, and v_2. They have already been globally optimized for PC by Götze and Voigtmann for dielectric, neutron-scattering, and depolarized light-scattering data covering a much larger range of frequencies than that of our Brillouin-scattering spectra. The parameters of $\phi_s(t)$ are Ω_s, ν_s, Δ_s, and V_s. (Note that varying the parameters of ϕ_s has no effect on ϕ.)

In this section, the Götze-Voigtmann schematic MCT model will be used to compute the memory function $m(\omega)$ of Eq. (3), taken as $m(\omega)=\Delta^2\phi_s(\omega)$, where Δ^2 is the coupling constant. (We note that this is the same procedure employed by Rufflé *et al.* [14], who used the simpler Sjögren model.)

B. MCT fitting procedure

Fitting the Brillouin spectra $I_{ISO}(\omega)$ with the two-correlator MCT model described above is technically more difficult and, therefore, less straightforward than the other two fitting procedures. This is because $m(\omega)=\Delta^2\phi_s(\omega)$ must first be obtained by solving and Fourier transforming the MCT equations [two sets of Eq. (15)], and then interpolated to match the frequencies of the $I_{ISO}(\omega)$ spectrum.

For the fits with the schematic MCT model, we began with the parameters obtained in the depolarized light-scattering (DLS) fits of Götze and Voigtmann, shown in their Fig. 1 [15]. Since the correlators ϕ_s computed with the parameters they used gave very good fits to the depolarized light-scattering spectra over nearly four decades in frequency, we tried to fit the Brillouin-scattering spectra using these same parameters. However, the α peaks of the DLS spectra are at lower frequencies than the corresponding τ_α^{LA} values, as seen in Fig. 1, where $\tau_\alpha^{DLS}\sim 5\,\tau_\alpha^{LA}$. We found that the position of the α peak in $\omega\phi_s''(\omega)$ is primarily determined by the coupling constant V_s in Eq. (14b). We, therefore, treated V_s as a free fitting parameter. All other MCT parameters were kept at their DLS values. We solved the MCT equations [Eqs. (15)] for selected values of V_s and the resulting $\phi_s(\omega)$, after multiplication by the (adjustable) coupling constant Δ^2, was taken as the memory function $m(\omega)$ in Eq. (3). A nonlinear least-squares analysis was then carried out in which I_0 and Δ^2 were the free parameters. This process was repeated with different values of V_s until the fit was optimized. (Note that in fitting their Brillouin spectra of $NaLiPO_3$ with the idealized two-correlator schematic Sjögren model, Rufflé *et al.* also treated V_s as a free parameter while the system parameters were fixed from neutron-scattering results [14].)

The MCT fits for $T=160$, 180, 200, 220, 240, 260, 280, 300, 320, and 350 K are shown in Fig. 10. (For $T\geqslant 300$ K, the MCT parameters other than V_s were obtained by extrapolation from lower temperatures.) The resulting values V_s and χ^2 for these fits are given in Table II (note that the V_s values for the Brillouin fits are systematically smaller than the depolarized light-scattering values V_s^{DLS}). The MCT fits are comparable to the hybrid fits, and have lower χ^2 values at some temperatures. For the lowest temperatures, the low-frequency region of the MCT fits is poor, reflecting the known limitations of the model for low frequencies at $T<T_C$ [27]. At temperatures above 280 K, the fits were not sensitive to the value of V_s for $V_s\lesssim 3.5$. This is because the α peak in $\omega m''(\omega)$ is then above the Brillouin line, and the shape of the memory function in the Brillouin range (1 to 15 GHz) is nearly independent of V_s. As seen in Table II, the value of the coupling parameter V_s decreases monotonically with increasing temperature as predicted by MCT.

For the temperatures 180, 200, 220, 240, and 260 K, the position of the α peak in $\omega m''(\omega)$ was sufficiently well determined by the fits to estimate the MCT α-relaxation time

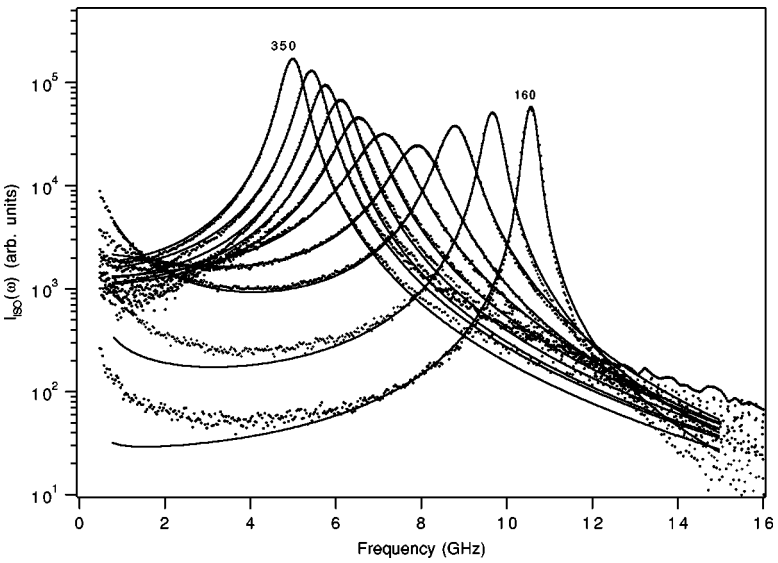

FIG. 10. Fits of PC $I_{ISO}(\omega)$ spectra with the extended schematic MCT model of Eqs. (15) and (14) for $T=350$, 320, 300, 280, 260, 240, 220, 200, 180, and 160 K. In the fits, $\gamma_0(T)=T/1000$ and $\omega_0(T)$ is fixed following Eq. (5). All MCT parameters are those found by Götze and Voigtmann from their fits to DLS spectra *except* for V_s, which has been adjusted to optimize the fits. For $T \geqslant 300$ K, the parameters other than V_s were determined by extrapolation from lower temperatures.

$\tau_\alpha = 1/\omega_\alpha$. The values found are listed in Table II and are also shown in Fig. 1 by the $*$ symbols. Note that the MCT values follow the same qualitative temperature dependence as the dielectric data, and are similar to (though somewhat lower than) the values we assumed for the hybrid fits. The ratio of τ_α (MCT) to τ_α of Eq. (1) increases monotonically with increasing temperature, from 0.14 at 180 K to 0.51 at 260 K. Thus, the MCT approach, in contrast to the other approaches described in the preceding two sections, is able to provide reasonable estimates of τ_α^{LA} purely on the basis of fits to the Brillouin spectra.

These results show that this extended schematic MCT model is able to simultaneously describe the spectra and also give reasonable fits for $\tau_\alpha(T)$, thus answering the question that originally motivated this study affirmatively.

VI. DISCUSSION AND CONCLUSIONS

As noted over 30 years ago by Montrose *et al.*, the detailed shape of the $I_{ISO}(\omega)$ Brillioun spectrum is relatively insensitive to the exact nature of the memory function [33]. This is due, as noted earlier, to the limited frequency range of Brillouin-scattering data. If ω_0 is fixed (from ultrasonic data), the ratio $m''(\omega_B)/m'(\omega_B)$ must have the ''correct'' value to obtain reasonable fits, but there is still enormous flexibility in constructing $m(\omega)$. If one wishes to extract meaningful information from the fits, then additional constraints must be imposed.

First, the α relaxation time should be reasonable. Fits using α-relaxation-only models, e.g., the Cole-Davidson function of Eq. (4), produce acceptable fits but give unreasonably short relaxation times at low temperatures. At $T \sim T_G$, one finds typically $\tau_\alpha^{CD}(T_G) \sim 10^{-7}$ s while other experimental techniques generally yield $\tau_\alpha(T_G) \sim 10^2$ s. This disagreement demonstrates the fact, already shown many times, that α-only models of structural relaxation are incomplete.

A great deal of research during the past 15 years has shown that structural relaxation occurs in two steps, starting with a fast decay towards a plateau that precedes the final α-relaxation process. Since the memory function $m(\omega)$ for longitudinal viscosity should also have this two-step form, the memory function used in the analysis of Brillouin-scattering spectra should include both the α-relaxation and the fast-relaxation regions of $m(\omega)$. If τ_α is constrained to follow the temperature dependence found in other measurements, such as dielectric or depolarized light-scattering spectroscopy, then the memory function must be extended to higher frequencies to provide sufficient damping once the α peak in $\omega m''(\omega)$ has moved below the Brillouin lines. This extension to include fast-relaxation processes can be implemented many ways, but most approaches require the introduction of a fast-β-relaxation time τ_β that does not correspond to the results of other experiments. In practice, there may also be other sources of fast relaxation—such as intramolecular vibrations—that influence the Brillouin spectra, but the high-frequency part of the structural relaxation dynamics must still be present.

Because the mode-coupling theory has been successful in analyzing a wide range of experimental data, we have used an empirical model for $m(\omega)$, which is qualitatively consistent with MCT. The hybrid model, which mimics the two-step relaxation scenario of MCT by combining the CD function for α relaxation with the critical-decay law (ω^a), has been shown to provide generally excellent fits to the Brillouin-scattering spectra.

Furthermore, we found that fixing $\beta=b=0.5$ produces fits of equally good quality as with $\beta=0.68$. [This value of $b=0.5$ follows, together with $a=0.29$, from fitting the minima of PC susceptibility spectra to Eq. (9).] Wiedersich *et al.* [28] have used this reduced hybrid model to fit their depolarized backscattering spectra of toluene; the reduction in the number of free fitting parameters relative to the usual procedure, where β and b are independent, represents an attractive variant of the hybrid model. It will be interesting to explore the ability of this model to simultaneously fit both depolarized backscattering spectra and Brillouin spectra for any given material.

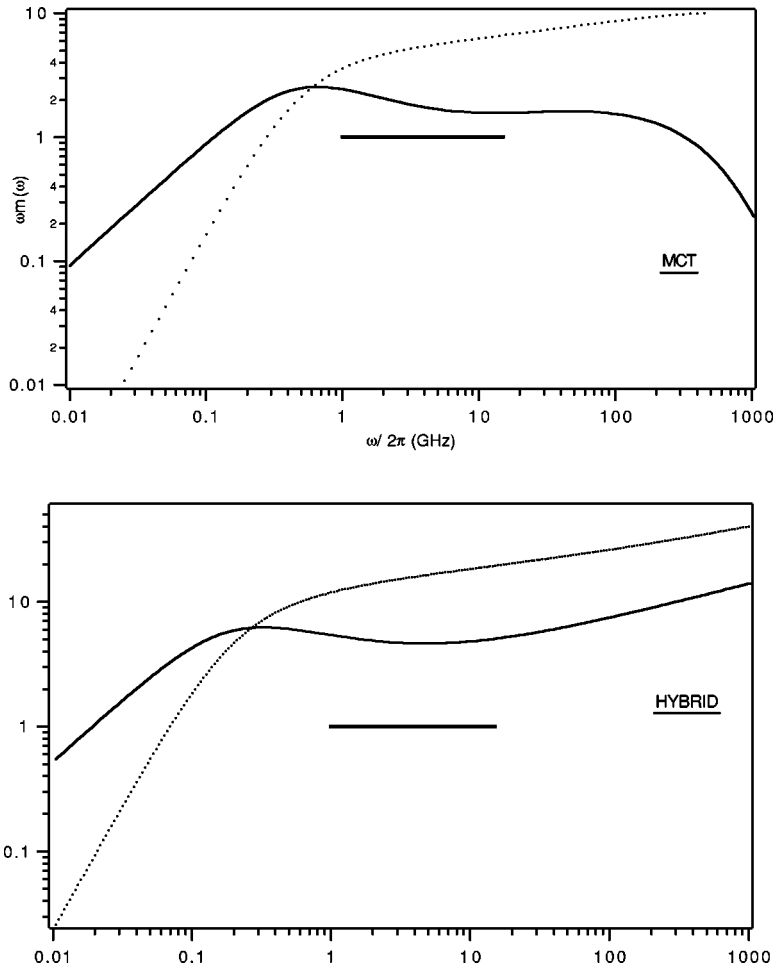

FIG. 11. $\omega m''(\omega)$ (solid lines) and $\omega m'(\omega)$ (broken lines) from the fits at 200 K. Top: MCT fit; bottom: hybrid fit with $\beta=b=0.5$ and $a=0.29$. The fit range (1–15 GHz) is indicated in both plots by a thick horizontal line.

We have also explored the applicability of the two-correlator schematic MCT model to the analysis of Brillouin spectra, a procedure first employed by Ruffl*é et al.* [14] who used the Sjögren model without hopping. We used the new extended model of Götze and Voigtmann [15] with which they fit depolarized light-scattering, neutron-scattering, and dielectric data for propylene carbonate with common parameters for the system correlator $\phi(t)$ for all the experiments. For the probe correlator $\phi_s(t)$, we kept the parameters Ω_s, ν_s, and Δ_s that they obtained from fits to depolarized light-scattering spectra fixed, but we varied V_s to optimize the fits to the Brillouin spectra, taking $m(\omega)=\Delta^2\phi_s(\omega)$, where Δ^2 is a free parameter. The resulting V_s values were systematically smaller [and the resulting frequency of the α peak in $\omega m''(\omega)$ higher] than those found from fits to the depolarized light-scattering spectra, consistent with the result that τ_α^{LA} is smaller than τ_α of depolarized light-scattering spectra as shown in Fig. 1. We then used the positions of the α peaks in the MCT memory function to estimate the relaxation time $\tau_\alpha^{MCT}=1/\omega_\alpha^{MCT}$. As seen in Fig. 1, the resulting τ_α^{MCT} values follow the temperature dependence expected on the basis of the dielectric data of Schneider *et al.* We emphasize that this MCT analysis is the only one of the three employed in this study that can provide a meaningful estimate of τ_α.

The recent Brillouin-scattering study of OTP by Monaco and co-workers [29,5,6,23] has suggested a different origin for the fast-relaxation process observed in Brillouin-scattering spectra: coupling of longitudinal acoustic modes to intramolecular degrees of freedom as originally suggested by Mountain [1]. Even in OTP, however, where this mechanism appears to be important, some part of the fast relaxation must be associated with structural relaxation.

Finally, we return to the question of the ability of Brillouin-scattering spectra to extract meaningful information about the structural relaxation process. In Fig. 11 we show $\omega m''(\omega)$ (solid lines) and $\omega m'(\omega)$ (broken lines) obtained from the MCT fits (top) and the hybrid fits with $\beta=b$ (bottom).

In the range of the Brillouin spectra (1–15 GHz indicated by the horizontal solid lines), the shapes of these curves are remarkably close, even though they were obtained with very different procedures. This result suggests that a reasonable phenomenological model such as the hybrid model, with the constraint that τ_α should have a temperature dependence consistent with that found by other techniques, can provide a credible representation of the memory function $m(\omega)$ characterizing the longitudinal viscosity.

ACKNOWLEDGMENTS

We thank W. Götze, J. Wiedersich, M. Fuchs, and R. Pick for helpful discussions and suggestions, Th. Voigtmann for

providing the computer programs (and extensive advice) for the schematic MCT analysis, and P. Lunkenheimer for providing the $\tau_\alpha(T)$ values shown in Fig. 1. H.Z.C. thanks the Alexander von Humboldt Foundation for support and the Technical University of Munich for hospitality during a visit when this project was begun. This research was supported by the National Science Foundation under Grant Nos. DMR-9616577 and DMR-9980370. Travel support for the CCNY-TUM collaboration was provided by NATO under Collaborative Research Grant No. CRG-930730.

APPENDIX: SOME MATHEMATICAL DETAILS

The normalized density fluctuation correlation function

$$\phi(t)=\langle\rho_q(0)\rho_q(t)\rangle/\langle|\rho_q(0)|^2\rangle \tag{A1}$$

obeys the generalized Langevin (or generalized oscillator) equation

$$\ddot{\phi}(t)+\gamma_0\dot{\phi}(t)+\omega_0^2\phi(t)+\int_0^t m(t-t')\dot{\phi}(t')dt'=0. \tag{A2}$$

We use the Laplace transform convention usually followed in the mode-coupling theory literature

$$F(z)=i\int_0^\infty e^{izt}F(t)dt \tag{A3}$$

with which we obtain

$$\phi(z)=\frac{-[z+m'(z)]-i[\gamma_0+m''(z)]}{[z^2-\omega_0^2+zm'(z)]+i[z\gamma_0+zm''(z)]}, \tag{A4}$$

where $m(z)=m'(z)+im''(z)$.

The power spectrum of the fluctuations in $\phi(t)$ is given by

$$S(\omega)=\mathrm{Im}[\phi(z)]_{z=\omega} \tag{A5}$$

and the light-scattering spectrum $I(\omega)\propto S(\omega)$ is then

$$I(\omega)=\frac{I_0[\gamma_0+m''(\omega)]}{[\omega^2-\omega_0^2+\omega m'(\omega)]^2+[\omega\gamma_0+\omega m''(\omega)]^2}, \tag{A6}$$

which is Eq. (3) in the text. (Note that without the i in Eq. (A3), m' and m'' would be exchanged, a convention that is frequently employed in the Brillouin-scattering literature.)

In the critical region preceding the α relaxation, $m(t)$ can be represented by

$$m_{crit}(t)=t^{-a}e^{-t/\tau_\alpha}, \tag{A7}$$

when the e^{-t/τ_α} cutoff factor prevents $m_{crit}(t)$ from adding to $m_\alpha(t)$ at frequencies below the center of the α-relaxation region. With Eq. (A3) and $m(\omega)=[m(z)]_{z=\omega}$, we have

$$m_{crit}(\omega)=i\int_0^\infty e^{i\omega t}t^{-a}e^{-t/\tau}dt, \tag{A8}$$

from which [34]

$$m_{crit}(\omega)=i\Gamma(1-a)\left(\frac{1}{\tau}-i\omega\right)^{a-1}. \tag{A9}$$

For the hybrid model, $m(\omega)=m_{CD}(\omega)+m_{crit}(\omega)$, so

$$\begin{aligned}\omega m(\omega)&=\Delta^2[(1-i\omega\tau)^{-\beta}-1]\\&\quad+i\omega B\Gamma(1-a)[\tau^{-1}-i\omega]^{a-1}\\&=\Delta^2[(1-i\omega\tau)^{-\beta}-1]\\&\quad+i\omega B\Gamma(1-a)\tau^{1-a}(1-i\omega\tau)^{a-1},\end{aligned} \tag{A10}$$

which is Eq. (7) in the text. [For $a=0.29$, $\Gamma(1-a)=1.282$.]

[1] R.D. Mountain, J. Res. Natl. Bur. Stand., Sect. A **70A**, 207 (1966); **72A**, 95 (1968).
[2] S. Loheider, G. Vogler, I. Petscherizin, M. Soltwisch, and D. Quitmann, J. Chem. Phys. **93**, 5436 (1990).
[3] H.Z. Cummins, G. Li, W.M. Du, and J. Hernandez, J. Non-Cryst. Solids **172-174**, 26 (1994).
[4] M. Soltwisch, G. Ruocco, B. Baushun, J. Bosse, V. Mazzacurati, and D. Quitmann, Phys. Rev. E **57**, 720 (1998).
[5] G. Monaco, S. Caponi, R. DiLeonardo, D. Fioretto, and G. Ruocco, Phys. Rev. E **62**, R7595 (2000).
[6] G. Monaco, D. Fioretto, L. Comez, and G. Ruocco, Phys. Rev. E **63**, 061502 (2001).
[7] M.J. Lebon, C. Dreyfus, Y. Guissani, R.M. Pick, and H.Z. Cummins, Z. Phys. B: Condens. Matter **103**, 433 (1997).
[8] W.M. Du, G. Li, H.Z. Cummins, M. Fuchs, J. Toulouse, and L.A. Knauss, Phys. Rev. E **49**, 2192 (1994).
[9] W.M. Du, Ph.D. dissertation, The City University of New York, 1996.
[10] A. Aouadi, C. Dreyfus, M. Massot, R.M. Pick, T. Berger, W. Steffen, A. Patkowski, and C. Alba-Simionesco, J. Chem. Phys. **112**, 9860 (2000).
[11] L. Sjögren, Phys. Rev. A **33**, 1254 (1986).
[12] T. Franosch, W. Götze, M.R. Mayr, and A.P. Singh, Phys. Rev. E **55**, 3183 (1997).
[13] A.P. Singh, G. Li, W. Götze, M. Fuchs, T. Franosch, and H.Z. Cummins, J. Non-Cryst. Solids **235-237**, 66 (1998).
[14] B. Ruffĺe, C. Ecolivet, and B. Toudic, Europhys. Lett. **45**, 591 (1999).
[15] W. Götze and Th. Voigtmann, Phys. Rev. E **61**, 4133 (2000).
[16] M. Frank, Diploma thesis, The Technical University of Munich, 2000.
[17] M. Elmroth, L. Borjesson, and L.M. Torell, Phys. Rev. Lett. **68**, 79 (1992).
[18] U. Schneider, P. Lunkenheimer, R. Brand, and A. Loidl, Phys. Rev. E **59**, 6924 (1999).
[19] D. Fioretto, L. Comez, G. Socino, L. Verdini, S. Corezzi, and

P.A. Rolla, Phys. Rev. E **59**, 1899 (1999); G. Monaco, L. Comez, and D. Fioretto, Philos. Mag. B **77**, 463 (1998).
[20] C.-H. Chung and S. Yip, Phys. Rev. A **4**, 928 (1971).
[21] J.P. Boon and S. Yip, *Molecular Hydrodynamics* (McGraw-Hill, New York, 1980).
[22] T. Scopigno, U. Balucani, G. Ruocco, and F. Sette, Phys. Rev. Lett. **85**, 4076 (2000).
[23] S. Mossa, G. Monaco, and G. Ruocco, e-print cond-mat/0104265.
[24] C. Dreyfus, A. Aouadi, R.M. Pick, T. Berger, A. Patkowski, and W. Steffen, Eur. Phys. J. B **9**, 401 (1999).
[25] A. Latz and M. Letz, Eur. Phys. J. B **19**, 323 (2001); T. Franosch, M. Fuchs, and A. Latz, Phys. Rev. E **63**, 061209 (2001).
[26] In carrying out fits to Eq. (3) with the memory functions $m(\omega)$ of Eqs. (4) or (7), we used the following conventions for units: ω, ω_0, γ_0, and Δ are all in GHz, while τ is in ns. In calculating $\omega\tau$, we, therefore, multiplied τ by 2π.
[27] W. Götze (private communication).
[28] J. Wiedersich, N. Surovtsev, and E. Rossler, J. Chem. Phys. **113**, 1143 (2000).
[29] G. Monaco, D. Fioretto, C. Masciovecchio, G. Ruocco, and F. Sette, Phys. Rev. Lett. **82**, 1776 (1999).
[30] W. Götze and L. Sjögren, Rep. Prog. Phys. **55**, 241 (1992).
[31] H.Z. Cummins, Y.H. Hwang, Gen Li, W.M. Du, W. Losert, and G.Q. Shen, J. Non-Cryst. Solids **235-237**, 254 (1998).
[32] N.J. Tao, G. Li, and H.Z. Cummins, Phys. Rev. Lett. **66**, 1334 (1991); W. Steffen, A. Patkowski, H. Gläser, G. Meier, and E.W. Fischer, Phys. Rev. E **49**, 2992 (1994); J. Gapinski, W. Steffen, A. Patkowski, A.P. Sokolov, A. Kisliuk, U. Buchenau, M. Russina, F. Mezei, and H. Schober, J. Chem. Phys. **110**, 2312 (1999); J. Wiedersich, T. Blochowicz, S. Benkhof, A. Kudlik, N.V. Surovtsev, C. Tschirwitz, V.N. Novikov, and E. Rössler, J. Phys.: Condens. Matter **11**, A147 (1999); A.P. Sokolov, A. Kisliuk, V.N. Novikov, and K. Ngai, Phys. Rev. B **63**, 172204 (2001); S. Adichtchev, St. Benkhof, Th. Blochowicz, E. Rössler, Ch. Tschirwitz, V. Novikov, and J. Wiedersich, Phys. Rev. Lett. **88**, 055703 (2002).
[33] C.J. Montrose, V.A. Solovyev, and T.A. Litovitz, J. Acoust. Soc. Am. **43**, 117 (1968).
[34] I.S. Gradshteyn and I.M. Ryzhik, in *Table of Integrals, Series, and Products*, 4th ed. (Academic Press, New York, 1965), p. 317.
[35] L. Simeral and R.L. Amey, J. Phys. Chem. **74**, 1443 (1970).
[36] J. Wuttke, M. Ohl, M. Goldhammer, S. Roth, U. Schneider, R. Lunkenheimer, R. Kahn, B. Rufflé, R. Lechner, and M.A. Berg, Phys. Rev. E **61**, 2730 (2000).
[37] R. Böhmer, K.L. Ngai, C.A. Angell, and D.J. Plazek, J. Chem. Phys. **99**, 4201 (1993).